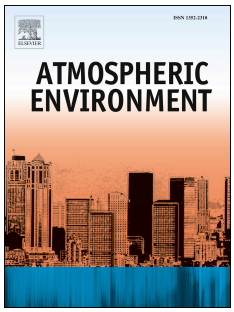

Exploring water-soluble organic aerosols structures in urban atmosphere using advanced solid-state ^{13}C NMR spectroscopy

Regina M.B.O. Duarte, Pu Duan, Jingdong Mao, Wenying Chu, Armando C. Duarte, Klaus Schmidt-Rohr

PII: S1352-2310(20)30240-5

DOI: https://doi.org/10.1016/j.atmosenv.2020.117503

Reference: AEA 117503

To appear in: *Atmospheric Environment*

Received Date: 29 October 2019

Revised Date: 8 April 2020

Accepted Date: 10 April 2020

Please cite this article as: Duarte, R.M.B.O., Duan, P., Mao, J., Chu, W., Duarte, A.C., Schmidt-Rohr, K., Exploring water-soluble organic aerosols structures in urban atmosphere using advanced solid-state ^{13}C NMR spectroscopy, *Atmospheric Environment* (2020), doi: https://doi.org/10.1016/j.atmosenv.2020.117503.

CRediT author statement

Regina M. B. O. Duarte: Conceptualization, Investigation, Resources, Formal analysis, Writing- Original draft preparation and Review & Editing, Funding acquisition, Project administration. **Pu Duan**: Data curation, Investigation, Formal analysis, Writing- Reviewing & Editing. **Jingdong Mao:** Conceptualization, Methodology, Validation, Writing - Review & Editing. **Wenying Chu:** Formal analysis, Writing- Reviewing & Editing. **Armando C. Duarte:** Visualization, Writing- Reviewing & Editing. **Klaus Schmidt-Rohr:** Methodology, Validation, Resources, Writing- Reviewing & Editing, Funding acquisition.

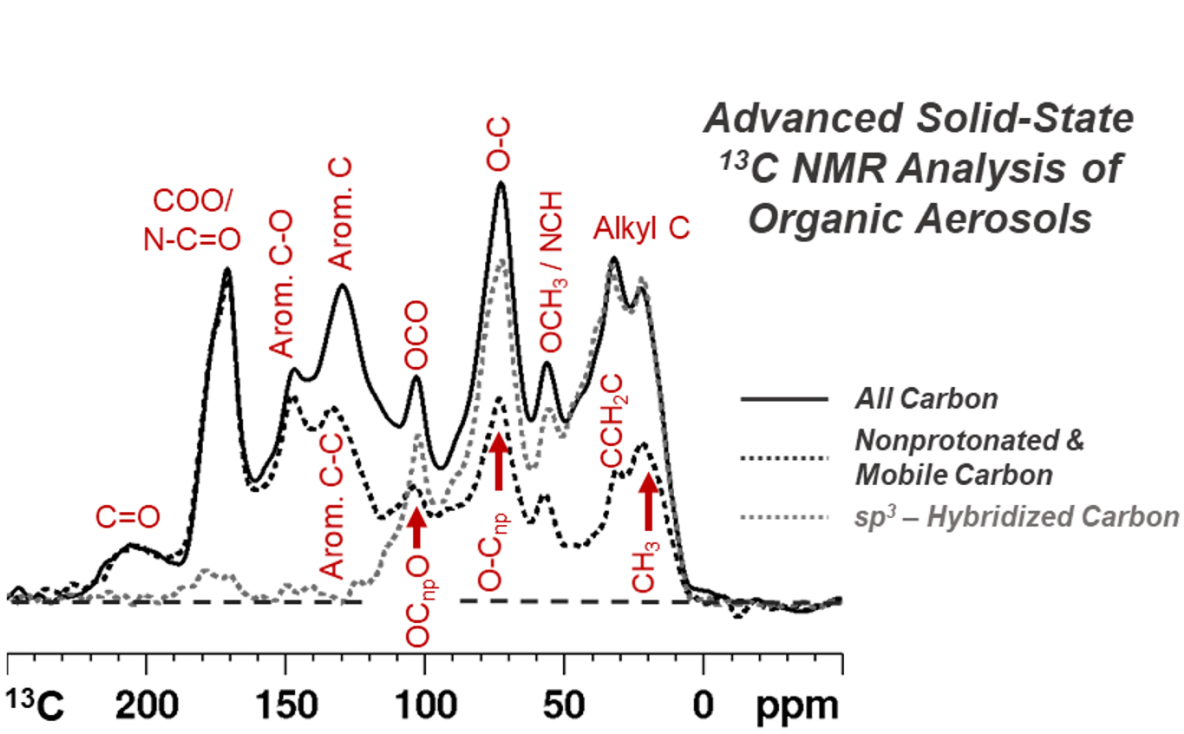

Exploring water-soluble organic aerosols structures in urban atmosphere using advanced solid-state ^{13}C NMR spectroscopy

Regina M. B. O. Duarte [a] *, Pu Duan [b], Jingdong Mao [c], Wenying Chu [c], Armando C. Duarte [a], Klaus Schmidt-Rohr [b]

[a] *Department of Chemistry & CESAM, University of Aveiro, 3810-193, Aveiro, Portugal*

[b] *Department of Chemistry, Brandeis University, 415 South Street, Waltham, MA 02453, USA*

[c] *Department of Chemistry and Biochemistry, Old Dominion University, 4541 Hampton Blvd, Norfolk, VA 23529, USA*

* Corresponding author: *E-mail:* regina.duarte@ua.pt; *Phone:* +351 234 370 200.

Abstract: Water-soluble organic matter (WSOM) in air particles has profound effects on climate and human health. At the heart of this environmental significance of WSOM lies a complex set of compounds, of which a major fraction still often remains undeciphered. Yet, not all environmental problems require delving into the molecular-level identification of WSOM constituents. Understanding the contribution of different functional groups to whole aerosol WSOM composition offers a highly important structural dataset that enables a better representation of WSOM in climate studies. For the first time, advanced solid-state ^{13}C nuclear magnetic resonance (NMR) techniques, including nearly quantitative ^{13}C multiple cross polarization/magic angle spinning (multiCP/MAS), multiCP/MAS with dipolar dephasing, multiCP/MAS with ^{13}C chemical shift anisotropy filter, and two-dimensional ^{1}H–^{13}C heteronuclear correlation (2D HETCOR), are applied to acquire an accurate quantitative structural description of whole aerosol WSOM collected in an urban atmosphere. Two urban aerosol WSOM samples collected in two short periods of time, under different wintry weather conditions, were investigated. NMR data successfully pinpointed the variability of whole aerosol WSOM composition, allowing to suggest source-specific structural characteristics for each sample in two short periods of time. A new structural model of urban aerosol WSOM was build based on this compositional data, showing the presence of three independent classes of compounds that vary both in content and

molecular diversity within short periods of time: heteroatom-rich aliphatic (either chain or branched), carbohydrate-like moieties, and highly substituted aromatic units. These findings establish advanced solid-state NMR as a promising tool for probing the chemical structures of inhomogeneous aerosol WSOM in rapidly changing atmospheric conditions, allowing to resolve discrepancies between modeled and measured aerosol WSOM.

Keywords: Water-soluble organic aerosols; Quantitative structural diversity; Structural model; Source assignment; Advanced solid-state ^{13}C NMR spectroscopy

1. Introduction

Water-soluble organic matter (WSOM) from fine particulate matter ($PM_{2.5}$, aerodynamic diameter less than 2.5 μm) plays a key role on climate, through its impact on cloud formation and properties (Müller et al., 2017; Padró et al., 2010), Earth's radiative balance (Laskin et al., 2015; Moise et al., 2015), and atmospheric chemistry (George et al., 2015; Laskin et al., 2015). Atmospheric deposition of aerosol WSOM can also affect carbon and nitrogen biogeochemical cycles in aquatic ecosystems (Iavorivska et al., 2016; Witkowska et al., 2016). Fine aerosol WSOM may also exert adverse health effects by generating reactive oxygen and nitrogen species (Tuet et al., 2016; Verma et al., 2014). Understanding these dynamic processes involving aerosol WSOM depends on how well one can identify its organic constituents. Yet, the ability to address such organic matrix is rather challenging, including $PM_{2.5}$ collection in amounts suitable for chemical analysis, WSOM extraction/processing ensuring representativeness of the extracted organic materials, complexity of WSOM composition, and limitations of some instrumental techniques to deal with such complexity (Duarte and Duarte, 2011). Keeping these challenges in mind, one must decide the level of structural and/or molecular knowledge required to answer a specific problem. In fact, most of the research on aerosol WSOM (e.g., optical properties, secondary formation, atmospheric variability, and source apportionment) only require intermediate levels of structural analysis, such as the identification of specific classes of compounds or functional groups (Nozière et al., 2015). Still, attaining this level of structural identification necessitates an understanding of the inherent complexity of WSOM composition, as well as its atmospheric fate and reactivity (Duarte and Duarte, 2015; Nozière et al., 2015).

Recent reviews have settled the debate regarding the use of different sophisticated analytical techniques to unravel the complex chemical composition of aerosol WSOM (Duarte and Duarte, 2017; Nozière et al., 2015). The remarkable advance of high-resolution analytical techniques, namely ultrahigh resolution mass spectrometry and solution-state multidimensional nuclear magnetic resonance (NMR) spectroscopy, has provided fundamentally novel insights into the structural composition of aerosol WSOM (Chalbot et al., 2013, 2016; Duarte et al., 2019, 2017a; Duarte and Duarte, 2017, 2011; Matos et al., 2017; Schmitt-Kopplin et al., 2010; Willoughby et al., 2016). Solution-state NMR methods have been particularly essential in clarifying some intricacies of the structure-origin relationships of different aerosol WSOM samples. However, these methods still have several shortcomings when dealing with complex organic mixtures (e.g., low sample solubility, non-detection of non-protonated carbons). A more comprehensive overview on these limitations is found in Simpson et al. (Simpson et al., 2011) and Mao et al. (Mao et al., 2017). Solid-state ^{13}C NMR, on the other hand, is an essential tool in overcoming some of those limitations in the untargeted structural analysis of complex mixtures (Mao et al., 2017). As described by Mao and co-workers (2017), when compared with solution-state NMR, solid-state NMR has the following advantages: (1) it overcomes sample solubility problems; (2) it requires less sample handling and is free of solvent effects; (3) it does not consume sample, thus allowing for its recovery for subsequent structural analysis; (4) it facilitates a much higher sample concentration than solution NMR, thus enhancing signals intensity; (5) it allows the straightforward detection of non-protonated carbons, allowing for the quantitative characterization of complex organic matrices; (6) the fast tumbling of molecules averages anisotropic interactions in solution NMR, while in solid-state NMR these anisotropic interactions can be manipulated with specially developed pulse sequences to extract structural information not available from solution NMR; (7) it can identify domains and heterogeneities within complex organic structures, which cannot be easily discerned by solution NMR; and (8) the macro-molecular structures, aggregates, and colloids present in complex organic mixtures slow the tumbling of these molecules, leading to T_2 relaxation times that are too short to allow many of the pulse sequences of solution NMR to be successfully used (Mao et al., 2017).

Yet, the application of solid-state ^{13}C NMR to aerosol WSOM analysis has been rather limited (Duarte et al., 2015, 2007; Sannigrahi et al., 2006), mostly due to the low atmospheric concentrations of aerosol WSOM, rendering the routine application of these methods difficult. When solid-state ^{13}C NMR

is used for aerosol WSOM characterization, the individual WSOM samples are usually pooled together according to different pollution or seasonal events, aiming at obtain enough amount of sample for NMR analysis (30-80 mg) (Duarte et al., 2015, 2007, 2005; Sannigrahi et al., 2006). These composite aerosol WSOM samples typically represent average ambient and/or meteorological conditions (e.g. seasons or biomass burning events), which however do not allow for capturing the individual WSOM compositional changes in short periods of time (i.e., up to a week (Duarte and Duarte, 2017)), thus hindering the investigation of chemical processes or aerosol sources in rapidly changing scenarios (e.g., different air masses or changes in atmospheric boundary-layer height). Furthermore, the most frequently used technique has been the standard cross-polarization magic-angle spinning (CP/MAS) ^{13}C NMR experiment, which only provides a semi-quantitative assessment of the carbon functional group distributions within the studied samples. Advanced solid-state ^{13}C NMR methods (e.g., ^{13}C direct polarization/magic angle spinning (DP/MAS) and DP/MAS with recoupled dipolar dephasing, ^{13}C multiple cross polarization/MAS (multiCP/MAS) and multiCP/MAS with dipolar dephasing, ^{13}C chemical shift anisotropy (CSA) filter, and two-dimensional $^{1}H–^{13}C$ heteronuclear correlation (2D HETCOR) NMR) can cope with this complexity by successfully providing accurate and detailed structural data on complex organic mixtures, such as those from aquatic and soil samples. In this regard, readers are encouraged to consult the works of Johnson and Schmidt-Rohr (2014) and Mao et al. (2017, 2012, 2011), and references therein to obtain a more complete understanding of the advantages of advanced solid-state ^{13}C NMR methods over conventional CP/MAS ^{13}C NMR for the analysis of such complex organic materials (Johnson and Schmidt-Rohr, 2014; Mao et al., 2017, 2012, 2011). These advanced solid-state NMR methods have never been applied to the structural analysis of aerosol WSOM. Furthermore, little is known about the structural features of the aerosol WSOM as a whole, as an important fraction of this organic component still eludes the current analytical window.

This study took the challenge to explore the structural diversity of whole aerosol WSOM by applying for the first time advanced solid-state ^{13}C NMR techniques. A standard reference sample of urban air particles (NIST SRM® 1648a) and urban $PM_{2.5}$ WSOM samples collected under different weather conditions during two consecutive weeks in winter were selected for this study. The NIST SRM® 1648a material was used as a surrogate for urban $PM_{2.5}$ samples to assess whether the whole atmospheric particulate matter was amenable to advanced solid-state ^{13}C NMR analysis. The objectives were: (i) to assess the effectiveness of advanced solid-state ^{13}C NMR for the analysis of

organic aerosols, (ii) to acquire a comprehensive structural description of whole aerosol WSOM, (iii) to quantify and assess the variability of the structural composition of whole aerosol WSOM in two short periods of time, (iv) to identify the potential sources of the major structural categories of aerosol WSOM, and (v) to build structural model representing the chemical diversity of urban aerosol WSOM. The level of structural details here attained breaks the solid-state NMR resolution barrier on the spectral identification of specific chemical classes in ambient organic aerosols, allowing the accurate assessment of the atmospheric concentrations of the major and specific functional groups of these highly complex atmospheric matrices on relatively short periods of time.

2. Materials and methods

2.1. Sampling and extraction of aerosol WSOM samples

The $PM_{2.5}$ samples were collected on a rooftop (ca. 20 m above ground) at the campus of University of Aveiro (40°38'N, 8°39'W), which is located about 10 km from the Atlantic coast on the outskirts of the city of Aveiro. The sampling site is impacted by both marine air masses travelling from the Atlantic Ocean and anthropogenic emissions from vehicular transport, residential, and industrial sources (Duarte et al., 2019, 2017b; Matos et al., 2017). Episodes of increased $PM_{2.5}$ and WSOM concentrations are common in this area during colder seasons and they can last several days (Duarte et al., 2019, 2017b, 2015), allowing the collection of enough amount of aerosol WSOM within relatively short periods of time for subsequent NMR studies. Each $PM_{2.5}$ sample was collected on a weekly basis (i.e., 7 days in continuum) in the periods of 4-11 February 2015 (Sample S1, start/end time: 15:35) and 11-18 February 2015 (Sample S2, start/end time: 15:50), on pre-fired (at 500 °C) quartz-fiber filters (20.3×25.4 cm; Whatman QM-A, Maidstone, UK) with an airflow rate of 1.13 m^3 min^{-1}. Additional details on aerosol sampling procedure are available in Section S1, in Supplementary Material (SM) data. After sampling, the filter samples were folded in two, wrapped in aluminum foil and immediately transported to the laboratory, where they were weighted and stored frozen until further analysis. The meteorological data recorded during the $PM_{2.5}$ samples collection are available in Table S1, in SM.

An area of 315 cm^2 of each collected filter was extracted with 150 mL of ultra-pure water, and the dissolved organic carbon (DOC) content of each aqueous extract was measured by means of a Shimadzu (Kyoto, Japan) TOC-5000A Analyzer. Additional details on water-soluble organic carbon

(WSOC) extraction and DOC analysis can be found in Section S2, in the SM. The WSOC concentrations are expressed in μg C m^{-3} (additional details are available in Table S2, in SM). After the WSOC extraction, each aqueous aerosol extract was freeze-dried, and the obtained solid residues (designated as "whole aerosol WSOM samples") were kept in a desiccator over silica gel until the solid-state NMR analysis.

2.2. Advanced solid-state ^{13}C NMR spectroscopy

All the NMR experiments were performed at 100 MHz for ^{13}C and 400 MHz for ^{1}H using a Bruker Avance 400 spectrometer. Solid NIST SRM® 1648a material and aerosol WSOM samples were packed in 4-mm-diameter zirconia rotors with Kel-F caps, and experiments were run in a double-resonance probe head. The ^{13}C chemical shifts were referenced externally to tetramethylsilane (TMS), with $^{13}COO^-$ labeled glycine at 176.49 ppm as a secondary reference. Quantitative ^{13}C NMR spectra were acquired using direct polarization (DP), 14 kHz magic-angle spinning (MAS), and a recycle delay of 20 s for NIST SRM® 1648a (approximately 90 mg), 1 s for aerosol WSOM sample S1 (approximately 32 mg), and 4 s for aerosol WSOM sample S2 (approximately 80 mg). The acquired ^{13}C DP/MAS NMR spectra are shown in Section S3, Figure S1, in the SM. Urban aerosol WSOM samples S1 and S2 were further characterized using nearly quantitative multiple cross-polarization magic angle spinning (multiCP/MAS) ^{13}C NMR, multiCP/MAS ^{13}C NMR with dipolar dephasing, and multiCP/MAS with a ^{13}C chemical shift anisotropy (CSA) filter. The nearly quantitative multiCP/MAS ^{13}C spectra were collected at a spinning speed of 14 kHz, with very small (<3%) spinning sidebands that have minimal overlap with centerbands. The 90° ^{13}C pulse length was 4.2 μs (Johnson and Schmidt-Rohr, 2014). The multiCP/MAS experiment combined with dipolar dephasing was applied to obtain quantitative structural information on non-protonated carbons and mobile segments. Most of the experimental conditions were the same as for the multiCP/MAS method except that a recoupled dipolar dephasing time of 68 μs was applied (Mao and Schmidt-Rohr, 2004a). The ^{13}C CSA filter was used to separate signals of sp^3-hybridized carbons from those of sp^2- and sp-hybridized carbons (i.e., to resolve the overlap between anomeric and aromatic carbon signals). This technique is based on the carbon bonding symmetry, which results in CSAs of sp^3-hybridized carbons being much smaller than those of sp^2- and sp-hybridized carbons, so their magnetization remains after a certain recoupling time (Mao and Schmidt-Rohr, 2004b).

Sample S2 was further characterized by means of two-dimensional ^{1}H-^{13}C heteronuclear correlation (2D HETCOR) NMR. In the 2D HETCOR spectrum, specific functional groups and their connectivities and proximity can be identified (Mao et al., 2001). 2D HETCOR experiments were performed at a spinning speed of 7.5 kHz. Standard Hartmann-Hahn CP (HH-CP) with 0.5 ms CP time was used, allowing for correlations between carbons and protons within ~0.5 nm radius. Sample S1 was not analyzed by means of 2D HETCOR due to its small mass amount (approximately 32 mg) and correspondingly low signal-to-noise ratio.

3. Results and discussion

3.1. Contribution of WSOM to $PM_{2.5}$ mass

The ambient concentrations of $PM_{2.5}$, water-soluble organic carbon (WSOC), and total mass of WSOM follow the same weekly trend, with higher values during the first week (Table 1). During this period, the inflowing air masses mostly come from inland (Table S1, SM), containing presumably a higher content of particulate organics from both local and continental sources. These conditions contrast with the cleaner air masses originating from the ocean sector during the second week, which usually contain a lower amount of particulate organic matter. Overall, the WSOM accounts to 23.4-25.3% of the urban $PM_{2.5}$ mass during the two sampling periods, being within the range of variation previously reported for this same location in winter (Duarte et al., 2017a).

Table 1. Ambient concentrations of $PM_{2.5}$, WSOC, total mass of particulate WSOM, and WSOM/$PM_{2.5}$ mass ratio in each sampling period.

Parameter	Sample S1	Sample S2
Total $PM_{2.5}$ (μg m^{-3})	22.7	16.9
WSOC (μg C m^{-3})	3.32 ± 0.08	2.67 ± 0.04
WSOM [(a)] (μg m^{-3})	5.31 ± 0.26	4.28 ± 0.10
WSOM/$PM_{2.5}$ (%)	23.4	25.3

[(a)] [WSOM] = [WSOC] × 1.6 (factor used to convert WSOC into WSOM derived from elemental analysis of WSOC aerosol samples collected during different seasons at Aveiro (Duarte et al., 2015)).

3.2. Qualitative and quantitative NMR analysis of aerosol WSOM

Figures 1(a) and 1(b) shows the nearly quantitative multiple cross-polarization magic angle spinning (multiCP/MAS) ^{13}C NMR spectra of aerosol WSOM samples S1 and S2, respectively. The

corresponding dipolar-dephased 68-µs ^{13}C multiCP/MAS NMR spectra are shown in Figures 1(c) and 1(d), whereas the ^{13}C multiCP/MAS spectra after a 13C chemical shift anisotropy (CSA) filter are displayed in Figures 1(e) and 1(f). The quantitative direct polarization magic angle spinning (DP/MAS) ^{13}C NMR spectra of the aerosol WSOM samples and NIST SRM® 1648a material are shown in Figure S1 (SM). The higher noise level in the DP spectra, particularly of sample S1, hinders the detection of smaller peaks, which are more clearly observed in the corresponding multiCP spectra due to their better signal-to-noise ratio. The presence of large spinning sidebands in the DP spectrum of NIST SRM® 1648a, which are also seen in the corresponding ^{1}H NMR spectrum (Figure S2, SM), are likely due to dipolar fields of paramagnetic species in this sample; this is supported by the presence of iron in the sample (3.92 ± 0.21%, certified mass fraction). This feature indicates the need to minimize the amount of paramagnetic species in the sample, which is the case for WSOM samples S1 and S2.

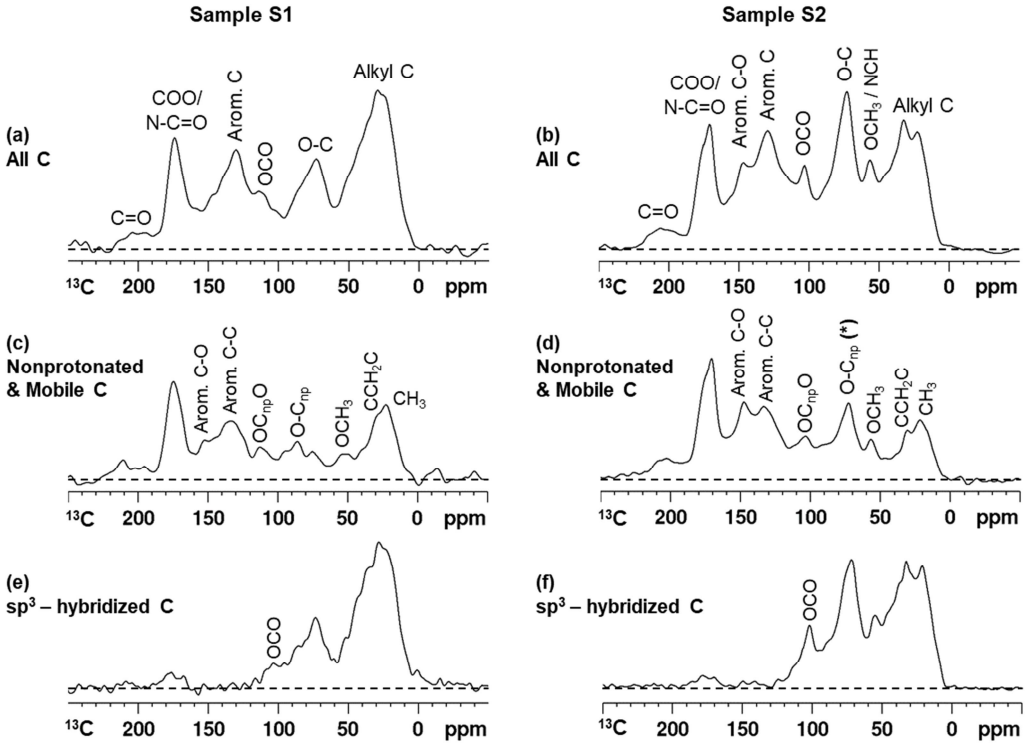

Figure 1. ^{13}C NMR with spectral editing of whole WSOM extracted from urban $PM_{2.5}$ sample S1 [(a), (c), and (e)] and sample S2 [(b), (d), and (f)] collected in Aveiro. (a, b) Nearly quantitative multiCP/MAS ^{13}C NMR spectra (all carbon (C)), compared to the corresponding (c, d) dipolar-dephased 68-µs multiCP/MAS ^{13}C NMR spectra of nonprotonated C (C_{np}) and highly mobile CH_n groups, and (e, f) selection of sp^3-hybridized C signals by a ^{13}C CSA filter. The asterisk (*) in (d) denotes that the resonance at 62–94 ppm can have contributions of both O-C_{np} and highly mobile O–C(H,R')–C groups.

Table 2 lists the integrals of the NMR resonances of the specific functional groups identified in WSOM samples S1 and S2 by means of the multiCP and spectral-editing techniques as well as their ambient concentrations. The assignments are as follows: 0−49 ppm, alkyl carbon (C); 49−62 ppm, NCH and OCH_3; 62−94 ppm, O-alkyl C, including carbohydrate-like C; 94−110 ppm, O−C−O anomeric C; 110−141 ppm, aromatic C-C and C-H; 141−160 ppm, aromatic C−O; 160−188 ppm, COO and N−C=O; and 188−230 ppm, ketone or aldehyde C. The spectra of multiCP/MAS ^{13}C NMR combined with dipolar dephasing selected nonprotonated carbons and mobile functional groups, providing remarkable information on the type of potential functionalities within the two aerosol WSOM samples. The NMR data indicate that these samples hold similar carbon functional groups; however, they differ in terms of the relative carbon distribution.

Table 2. Integration results (percentage values) based on multiCP/MAS ^{13}C NMR and spectral editing techniques, and ambient concentrations (in µg C m^{-3}) of each carbon functional group.

Sample ID	Chemical Shifts (ppm) and Assignments										
	230–188	188–160	160–141	141–110		110–94	94–62		62–49		49–0
	R(C=O)H R(C=O)R'	COO N-C=O	Arom. C–O	Arom. C-C	Arom. C-H	O–C(R,R')–O O–C(H,R')–O	O–C(R,R')–C and mobile O–C(H,R')–C	O–C(H,R')–C and O–CH_2–C	OCH_3	NCH	CCH_2C CCH_3
Percentage (%)											
S1	2.8	13.4	4.6	14.6	4.8	3.8	7.2	9.7	4.0	3.4	31.8
S2	3.6	12.4	8.4	15.4	2.9	6.9	10.5	9.5	3.8	2.3	24.3
Ambient concentration [(a)] (µg C m^{-3})											
S1	0.09	0.44	0.15	0.48	0.16	0.13	0.24	0.32	0.13	0.11	1.06
S2	0.10	0.33	0.23	0.41	0.08	0.18	0.28	0.25	0.10	0.06	0.65

[(a)] Ambient concentration of each carbon functional group calculated based on the corresponding integration result (percentage value) and on the total amount of WSOC of the sample (shown in Table 1).

The spectrum of sample S1 is clearly dominated by the resonance assigned to alkyl C (31.8%), whereas the alkyl C (24.3%) and O-alkyl C (20.0%) resonances dominate the spectrum of sample S2 (Table 2). The NMR resonance assigned to carbohydrate-like moieties or other O-alkyls (62−94 ppm) is quite intense in both spectra (16.9 and 20.0%, respectively), particularly when compared to data obtained in previous conventional CP/MAS ^{13}C NMR spectra of urban aerosol WSOM from cold seasons (10-12% of the total NMR peak area) (Duarte et al., 2015). The difference between these data and those previously published could be due to the different experimental procedures applied to

WSOM processing (Duarte et al., 2015). Previously, the WSOM samples were isolated from the water-soluble inorganics using a solid-phase extraction (SPE) procedure (Duarte et al., 2015), whereas the present study focus on whole aerosol water-soluble extracts. It is suggested that the WSOM isolated using SPE is enriched in those organic species that are targeted by the low hydrophilic character of the SPE sorbent, which retains the highly conjugated and more hydrophobic compounds of the aerosol WSOM (Duarte et al., 2015). The spectral features reported here further suggest that carbohydrate-like moieties or other O-alkyl groups may contribute more than previously expected to the compositional features of whole aerosol WSOM in winter.

The aromatic C structures (110-160 ppm), of which a substantial portion are nonprotonated aromatic C-C (14.6 and 15.4% in samples S1 and S2, respectively), also have an important contribution to the compositional features of both WSOM samples. However, a closer inspection of the multiCP/MAS ^{13}C NMR data suggests that these aromatic C structures may have different origins in each sample. Note that the multiCP/MAS ^{13}C spectra of both samples exhibit two distinctive NMR resonances at 56 ppm (OCH_3 and NCH) and 146 ppm (aromatic C-O; e.g., -OCH_3 or -OH substituents), whose presence are typically assigned to lignin breakdown products (e.g., methoxyphenols) emitted from wood combustion for home heating during cold temperatures (Duarte et al., 2017a, 2015; Matos et al., 2017). Nonetheless, the contribution of aromatic C-O groups to sample S2 is 1.8 times higher than for sample S1. Furthermore, the -OCH_3 and NCH groups contribute equally to the resonance at 56 ppm in sample S1, whereas a major fraction of this resonance is assigned to -OCH_3 groups in sample S2. Moreover, the content in anomeric C groups (94-110 ppm), whose presence is usually attributed to carbohydrate-like structures emitted during the pyrolysis of cellulose and hemi-cellulose (Duarte et al., 2019, 2008; Matos et al., 2017), is also higher in sample S2 than in sample S1. These spectral findings suggest that sample S1 is less wood smoke impacted than sample S2, although biomass burning still contributes to the composition of the former sample. The question is now which possible additional sources can explain the content of both aromatic C-C and C-H groups in sample S1. Motor-vehicle exhaust and secondary organic aerosol (SOA) formation have been mentioned as possible additional sources of aromatic C groups to urban aerosol WSOM (Chalbot et al., 2014; Sannigrahi et al., 2006). For example, aromatic acids, such as phthalic acid and its isomer, terephthalic acid, as well as nitrophenyl-derived compounds and cinnamic acid are water-soluble secondary products of oxidation of aromatic hydrocarbons from traffic emissions (Chalbot et al., 2016, 2014; Hallquist et al., 2009; Lee

et al., 2014) and they have already been detected in aerosol WSOM samples in urban areas (Alier et al., 2013; Chalbot et al., 2016, 2014; Duarte et al., 2019, 2017a; Matos et al., 2017). Backward trajectories (Table S1) reveal that air masses transport from continental Europe was predominant during sample S1 collection, suggesting that the transport of polluted air masses from industrial and traffic-related urban sources (in addition to local sources) might contribute to the high aromatic C content of this WSOM sample. Fossil fuel combustions are also major sources of aliphatic compounds in urban atmospheres (Willoughby et al., 2016; Wozniak et al., 2012). The presence of traffic and industrial activity in short- and long-range proximity of the sampling location suggests that fossil fuel combustion is also a strong candidate for explaining the high content of saturated aliphatic C groups (0-49 ppm) in sample S1 (Table 2).

Approximately 17% (sample S1) to 20% (sample S2) of NMR signal intensity falls in the O-alkyl C region (62-94 ppm). Nevertheless, the estimates of protonated and nonprotonated O-alkyl C structures (Table 2) resonating within this region should be viewed with caution, as an uncounted fraction of O–C(H,R')–C resonating at ~73 ppm is highly mobile due to sample hygroscopicity. The O-alkyl C region is typically assigned to carbohydrate-like moieties, although other alcohols (polyols) can resonate within this region as well. Polyols have already been detected in urban aerosol WSOM (Fu et al., 2010; Minguillón et al., 2016; Suzuki et al., 2001; Wang and Kawamura, 2005) and are thought to be produced via photooxidation of isoprene in aerosols (e.g., 2-methyltetrols) (Fu et al., 2010; Minguillón et al., 2016). Carbohydrate-like moieties, on the other hand, are important components of aerosol WSOM and may include mono- and disaccharides (such as glucose, trehalose, maltose, fructose, and sucrose) and anhydrosugars (such as levoglucosan and mannosan) (Matos et al., 2017; Yttri et al., 2007). Glucose, fructose, maltose, and sucrose can be emitted from the combustion of cellulose and hemi-cellulose, whereas anhydrosugars are molecular markers of biomass burning emissions (Chalbot et al., 2013; Duarte et al., 2019, 2008; Matos et al., 2017). Primary saccharides, such as glucose and trehalose, may also reflect the contribution of biogenic sources (e.g., products of fungal metabolism) (Côté et al., 2008). Trehalose is considered a useful tracer of soil materials and associated microbiota (Simoneit et al., 2004) and, therefore, resuspension of soil from agricultural activities in areas near the sampling area could be a plausible source as well.

Interestingly, the content in NCH groups, which overlap with those of -OCH_3 groups in the multiCP ^{13}C NMR spectra and are removed by dipolar dephasing (Mao et al., 2012), is somewhat higher in sample

S1 than in sample S2 (Table 2). The presence of N-alkyl structures has already been identified in aerosol WSOM samples (Matos et al., 2017), but their quantification in organic aerosols is rather difficult. These N-containing organic structures could be associated with SOA formation, resulting from photochemical oxidation of different anthropogenic and natural gas-phase precursors (e.g., alkanes, carbonyl, aliphatic amines, epoxides, and anhydrides) (Duarte et al., 2019; Matos et al., 2017). The long-range transport of polluted air masses from inland urban and industrial sources (Table S1) can contribute to the higher content of these N-containing structures in sample S1 as compared to sample S2.

In both samples, the dipolar-dephased spectra also exhibit signals from -COO and N−C=O between 160−188 ppm, and ketones between 188−230 ppm. Apparently, the presence of aldehydes C groups (188-230 ppm) is not significant for both WSOM samples, since the corresponding dipolar-dephased spectra do not show a considerable signal decrease within this spectral region.

3.3. Structural information on aerosol WSOM from 2D HETCOR NMR

To further assess the connectivities (or proximities) of the different C functional groups, the 2D HETCOR spectrum of sample S2 was also acquired [Figure 2(a)]. The ^{1}H cross sections at specific ^{13}C chemical shifts were extracted to facilitate the identification of connectivities and/or proximities of different functional groups [Figure 2(b)]. The ^{1}H cross sections extracted at the alkyl ^{13}C chemical shifts of 21 and 33 ppm, attributable to mobile -CH_3 and CCH_2C groups, respectively, show that the dominant contributions are from alkyl ^{1}H at 1.2 ppm, although proximity to aromatic ^{1}H at 7.1 ppm is also observed, particularly for alkyl ^{13}C at 21 ppm. While the former feature indicates that polymethylene structures and terminal CH_3 are important contributors to WSOM, the latter indicates that neutral alkyl C groups (namely CH_3) might be also substituents in aromatic rings. The ^{1}H slice extracted at 42 ppm, likely from -CCHC and/or quaternary C groups, mainly show correlation with alkyl ^{1}H at 1.9 ppm, indicating that aliphatic structures in the WSOM sample may also include branched carbon chains.

The ^{1}H spectrum associated with OCH_3/NCH groups at 55 ppm indicates that these carbons are mainly associated with their directly bonded ^{1}H at 3.25 ppm, although their proximity with aromatic ^{1}H resonating at ≈8.0 ppm is also observed. Considering that -OCH_3 groups account for most of the resonance within the 49-62 ppm region (Table 2), these spectral features are consistent with the

presence of lignin-derived structures, which are a defining feature of biomass burning emissions and of importance in the composition of sample S2. The ^{1}H slice at the ^{13}C chemical shift of 71 ppm, assigned to -OCH groups, show mainly an O-alkyl ^{1}H band at 3.9 ppm, suggesting that these carbon sites primarily correlate with their directly bonded O-alkyl ^{1}H. Furthermore, the ^{1}H slice extracted at 102 ppm also indicates that the protonated anomeric C (O-C-O) shows correlations predominantly with anomeric ^{1}H resonating at 4.7 ppm. These findings confirm that both -OCH and O-C-O are primarily associated with carbohydrate-like moieties, whose presence in this sample may result from cellulose and hemicellulose combustion.

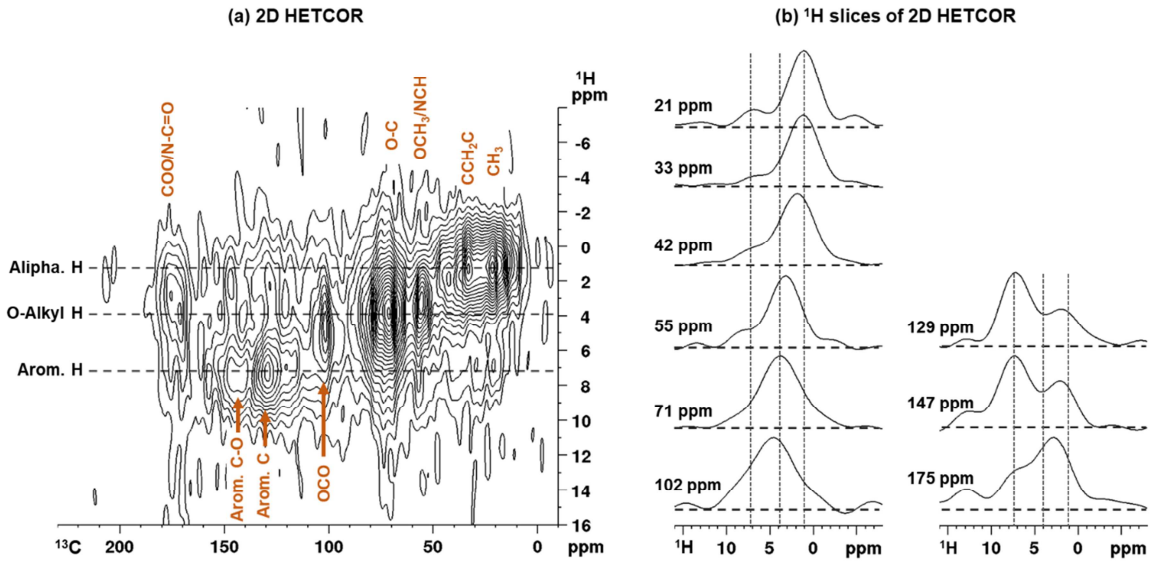

Figure 2. 2D $^{1}H-^{13}C$ HETCOR NMR spectrum (a) and associated ^{1}H slices (b) of whole WSOM extracted from $PM_{2.5}$ sample S2.

Within the aromatic NMR region, the ^{1}H slices extracted at the chemical shifts of aromatic C (129 ppm) and aromatic C-O (147 ppm) show major contributions from aromatic ^{1}H (at ≈7.3 ppm) as well as signals of alkyl ^{1}H (at ≈2.0 ppm). Aromatic C-O is also correlated with carboxylic acid ^{1}H at 12 ppm. These NMR fingerprints suggest the presence of highly substituted aromatic rings, bearing neutral (alkyl C) and/or O-containing (namely, OCH_3, OH, and/or COOR, where R=H or alkyl group) substituents. Such aromatic structural signatures are consistent with those observed for molecular markers of primary organic aerosols that are directly emitted from biomass burning (Duarte et al., 2019, 2008; Matos et al., 2017). Their presence in sample S2 confirm the importance of this emission source in the chemical composition of this aerosol WSOM sample during winter. Additional sources contributing to the aromatic structural signatures of sample S2 can also include *in-situ* secondary formation, as the presence of COO-bonded aromatics has been associated to terephthalic acid and

365 cinnamic acid, possibly formed during the oxidation of aromatic hydrocarbons from urban traffic
366 emissions (Duarte et al., 2019; Matos et al., 2017).
367 The 2D HETCOR spectrum also shows that COO/N−C=O groups (175 ppm), which account to 12% of
368 the NMR signal (Table 2), are primarily correlated with alkyl ^{1}H at 2.8 ppm, with additional
369 contributions from O-alkyl, aromatic and carboxylic acid ^{1}H. The presence of COO groups bonded to
370 alkyls, O-alkyls, and aromatic structures in urban aerosol WSOM can be attributed to SOA that form
371 via oxidation reactions involving naturally (e.g., sea-to-air emission of marine organics, and terrestrial
372 vegetation (Liu et al., 2011; Russell et al., 2011; Schmitt-Kopplin et al., 2012)) and anthropogenically
373 (e.g., biomass burning and fossil fuel combustion (Kundu et al., 2010; Liu et al., 2011)) gas-phase
374 precursors. In the context of the studied urban area, the contribution of fossil fuel SOA to total organic
375 aerosol load has a noteworthy importance in winter (up to 20% of the total aerosol carbon (Gelencsér
376 et al., 2007)), thus making atmospheric aging of anthropogenic volatile and semi-volatile organic
377 compounds a key process in defining the molecular features of urban organic aerosols.
378 A structural model of aerosol WSOM can be further deduced based on the data from multiCP/MAS ^{13}C
379 NMR with spectral editing techniques (Table 2) and 2D HETCOR. Figure 3 integrates all the structural
380 information on the complex molecular WSOM assemblies, with the addition of the chemical data from
381 2D solution-state NMR of urban organic aerosols (Duarte et al., 2019, 2017a; Matos et al., 2017). The
382 model shows that urban particulate WSOM contain at least three classes of compounds which are not
383 associated with each other in the same structure, and that vary both in concentration and molecular
384 diversity within short periods of time: (1) a core of heteroatom-rich aliphatics (either chain or branched,
385 mostly with $-CH_3$ and/or -COO terminal units), reflecting the large contribution of these structures as
386 deduced from the quantitative NMR data in Table 2; (2) carbohydrate-like moieties; and (3) highly
387 substituted aromatic units.
388

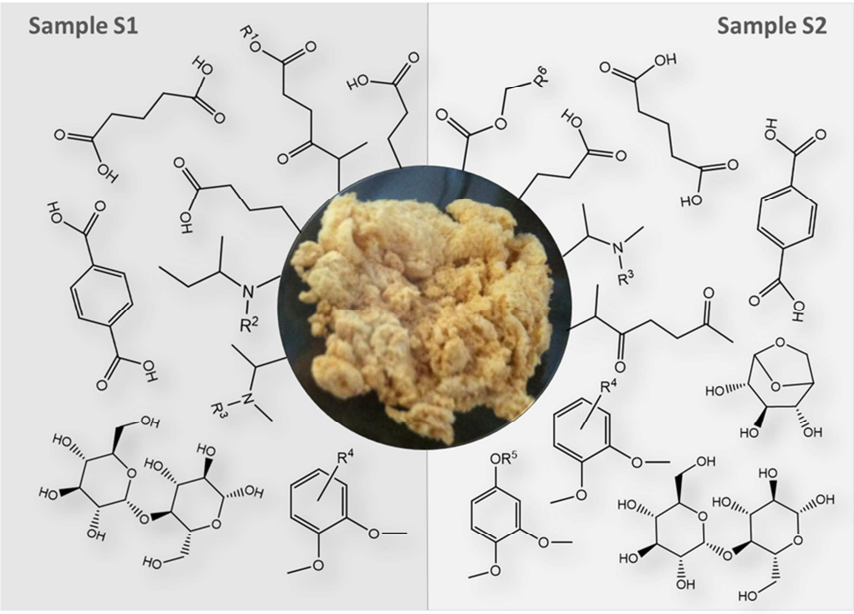

Figure 3. Structural model of aerosol WSOM in samples S1 and S2, with a ratio of aliphatic -CH_3, C-CH_2-C, -COO, aromatic C-O, and anomeric O-C-O of 5:11:7:2:2 and 4:8:6:4:3, respectively, as deduced from the combination of multiCP/MAS ^{13}C NMR with spectral editing techniques and 2D HETCOR (R^1 to R^6 = H or alkyl group; photo: aerosol WSOM, after freeze-drying).

4. Conclusions

The combination of multiCP/MAS ^{13}C NMR with spectral editing techniques has been critical in providing, for the first time, key information on the major and specific structural components of whole WSOM present in urban $PM_{2.5}$ collected in two short periods of time. The weekly-resolved structural data show quantifiable changes in whole aerosol WSOM composition not observable until now in NMR datasets provided in the literature. The O- and N-containing aliphatic features of sample S1 may reflect the effect of long-range-transported anthropogenic emissions (namely, from fossil-fuel combustion sources) that underwent chemical aging along the transport. These aged anthropogenic emissions might also contribute to the aromatic C features of sample S1. However, local residential wood burning also contributes to the WSOM composition to a minor extent. On the other hand, the structural characteristics of sample S2, particularly the carbohydrate-like and the highly substituted aromatic moieties, are mainly apportioned to local biomass burning emissions. SOA formation from anthropogenic precursors emitted from local traffic sources can also contribute to whole aerosol WSOM during the second week.

The knowledge on the whole aerosol WSOM functional-group composition should also be helpful for predicting the role of this fraction in diverse atmospheric processes. Rather than using surrogate organic compounds to represent aerosol WSOM, improved reproductions of how WSOM affect aerosol hygroscopic growth and activation should be obtained if accurate ambient concentrations of each carbon functional group (Table 2) are appropriately taken into account in such modelling studies (McNeill, 2015; Mircea et al., 2005). Our structural findings further highlight a dynamic picture of aerosol WSOM composition that should be integrated in climate models. For example, Martin and co-workers reported that it is not possible to use the same value of hygroscopicity for freshly emitted and aged soot particles in climate models due to their different chemical composition (Martin et al., 2013). Therefore, it is worth investigating how the hygroscopic properties change relative to the different composition of locally emitted primary organic aerosols and chemically processed organic particles, as this would make the inferred values in climate models more representative.

Future research should refine both the composition and structures of whole aerosol WSOM by addressing additional sample sets from other locations across different time scales, which should enable a more definite quantification and better constrained structural models of this organic aerosol fraction. The application of advanced solid-state ^{13}C NMR methods will lay the groundwork for such structure–function investigations, thus enabling exploration of role of WSOM in different atmospheric processes.

Acknowledgments

Thanks are due to FCT/MCTES for the financial support to CESAM (UID/AMB/50017/2019) and project AMBIEnCE (PTDC/CTA-AMB/28582/2017), through national funds. Regina Duarte also acknowledges financial support from FCT/MCTES (Investigator FCT Contract IF/00798/2015) and from the Fulbright Scholar Program (sponsored by the U.S. Department of State), as well as the Surface Ocean-Lower Atmosphere Study (SOLAS) for endorsing the AMBIEnCE project. The solid-state NMR spectrometer used in this work was funded by the NSF (Award No. 1726346). The authors also gratefully acknowledge the NOAA Air Resources Laboratory (ARL) for the provision of the HYSPLIT transport and dispersion model and/or READY website (http://www.ready.noaa.gov) used in this publication.

References

Alier, M., Van Drooge, B.L., Dall'Osto, M., Querol, X., Grimalt, J.O., Tauler, R., 2013. Source apportionment of submicron organic aerosol at an urban background and a road site in Barcelona (Spain) during SAPUSS. Atmospheric Chemistry and Physics 13, 10353–10371. https://doi.org/10.5194/acp-13-10353-2013

Chalbot, M.-C., Nikolich, G., Etyemezian, V., Dubois, D.W., King, J., Shafer, D., Gamboa da Costa, G., Hinton, J.F., Kavouras, I.G., 2013. Soil humic-like organic compounds in prescribed fire emissions using nuclear magnetic resonance spectroscopy. Environmental Pollution 181, 167–171. https://doi.org/10.1016/j.envpol.2013.06.008

Chalbot, M.-C.G., Brown, J., Chitranshi, P., Gamboa da Costa, G., Pollock, E.D., Kavouras, I.G., 2014. Functional characterization of the water-soluble organic carbon of size-fractionated aerosol in the southern Mississippi Valley. Atmospheric Chemistry and Physics 14, 6075–6088. https://doi.org/10.5194/acp-14-6075-2014

Chalbot, M.-C.G., Chitranshi, P., Gamboa da Costa, G., Pollock, E., Kavouras, I.G., 2016. Characterization of water-soluble organic matter in urban aerosol by 1H-NMR spectroscopy. Atmospheric Environment 128, 235–245. https://doi.org/10.1016/j.atmosenv.2015.12.067

Côté, V., Kos, G., Mortazavi, R., Ariya, P.A., 2008. Microbial and "de novo" transformation of dicarboxylic acids by three airborne fungi. Science of the Total Environment 390, 530–537. https://doi.org/10.1016/j.scitotenv.2007.10.035

Duarte, R.M.B.O., Duarte, A.C., 2017. NMR Studies of Organic Aerosols, in: Webb, G.A. (Ed.), Annual Reports on NMR Spectroscopy. Academic Press, Oxford, pp. 83–135. https://doi.org/10.1016/bs.arnmr.2017.04.003

Duarte, R.M.B.O., Duarte, A.C., 2015. Unraveling the structural features of organic aerosols by NMR spectroscopy: a review. Magnetic Resonance in Chemistry 53, 658–666. https://doi.org/10.1002/mrc.4227

Duarte, R.M.B.O., Duarte, A.C., 2011. A critical review of advanced analytical techniques for water-soluble organic matter from atmospheric aerosols. TrAC Trends in Analytical Chemistry 30, 1659–1671. https://doi.org/10.1016/j.trac.2011.04.020

Duarte, R.M.B.O., Freire, S.M.S.C., Duarte, A.C., 2015. Investigating the water-soluble organic functionality of urban aerosols using two-dimensional correlation of solid-state 13C NMR and

FTIR spectral data. Atmospheric Environment 116, 245–252. https://doi.org/10.1016/j.atmosenv.2015.06.043

Duarte, R.M.B.O., Matos, J.T.V., Paula, A.S., Lopes, S.P., Pereira, G., Vasconcellos, P., Gioda, A., Carreira, R., Silva, A.M.S., Duarte, A.C., Smichowski, P., Rojas, N., Sanchez-Ccoyllo, O., 2017a. Structural signatures of water-soluble organic aerosols in contrasting environments in South America and Western Europe. Environmental Pollution 227, 513–525. https://doi.org/10.1016/j.envpol.2017.05.011

Duarte, R.M.B.O., Matos, J.T.V., Paula, A.S., Lopes, S.P., Ribeiro, S., Santos, J.F., Patinha, C., da Silva, E.F., Soares, R., Duarte, A.C., 2017b. Tracing of aerosol sources in an urban environment using chemical, Sr isotope, and mineralogical characterization. Environmental Science and Pollution Research 24, 11006–11016. https://doi.org/10.1007/s11356-016-7793-8

Duarte, R.M.B.O., Piñeiro-Iglesias, M., López-Mahía, P., Muniategui-Lorenzo, S., Moreda-Piñeiro, J., Silva, A.M.S., Duarte, A.C., 2019. Comparative study of atmospheric water-soluble organic aerosols composition in contrasting suburban environments in the Iberian Peninsula Coast. Science of the Total Environment 648, 430–441. https://doi.org/10.1016/j.scitotenv.2018.08.171

Duarte, R.M.B.O., Pio, C.A., Duarte, A.C., 2005. Spectroscopic study of the water-soluble organic matter isolated from atmospheric aerosols collected under different atmospheric conditions. Analytica Chimica Acta 530, 7–14. https://doi.org/10.1016/j.aca.2004.08.049

Duarte, R.M.B.O., Santos, E.B.H., Pio, C.A., Duarte, A.C., 2007. Comparison of structural features of water-soluble organic matter from atmospheric aerosols with those of aquatic humic substances. Atmospheric Environment 41, 8100–8113. https://doi.org/10.1016/j.atmosenv.2007.06.034

Duarte, R.M.B.O., Silva, A.M.S., Duarte, A.C., 2008. Two-Dimensional NMR Studies of Water-Soluble Organic Matter in Atmospheric Aerosols. Environmental Science & Technology 42, 8224–8230. https://doi.org/Doi 10.1021/Es801298s

Fu, P.Q., Kawamura, K., Pavuluri, C.M., Swaminathan, T., Chen, J., 2010. Molecular characterization of urban organic aerosol in tropical India: Contributions of primary emissions and secondary photooxidation. Atmospheric Chemistry and Physics 10, 2663–2689. https://doi.org/10.5194/acp-10-2663-2010

Gelencsér, A., May, B., Simpson, D., Sánchez-Ochoa, A., Kasper-Giebl, A., Puxbaum, H., Caseiro, A., Pio, C.A., Legrand, M., 2007. Source apportionment of PM2.5 organic aerosol over Europe:

Primary/secondary, natural/anthropogenic, and fossil/biogenic origin. Journal of Geophysical Research Atmospheres 112, 1–12. https://doi.org/10.1029/2006JD008094

George, C., Ammann, M., D'Anna, B., Donaldson, D.J., Nizkorodov, S.A., 2015. Heterogeneous photochemistry in the atmosphere. Chemical Reviews 115, 4218–4258. https://doi.org/10.1021/cr500648z

Hallquist, M., Wenger, J.C., Baltensperger, U., Rudich, Y., Simpson, D., Claeys, M., Dommen, J., Donahue, N.M., George, C., Goldstein, A.H., Hamilton, J.F., Herrmann, H., Hoffmann, T., Iinuma, Y., Jang, M., Jenkin, M.E., Jimenez, J.L., Kiendler-Scharr, A., Maenhaut, W., McFiggans, G., Mentel, T.F., Monod, A., Prévôt, A.S.H., Seinfeld, J.H., Surratt, J.D., Szmigielski, R., Wildt, J., 2009. The formation, properties and impact of secondary organic aerosol: current and emerging issues. Atmospheric Chemistry and Physics 9, 5155–5236. https://doi.org/10.5194/acp-9-5155-2009

Iavorivska, L., Boyer, E.W., DeWalle, D.R., 2016. Atmospheric deposition of organic carbon via precipitation. Atmospheric Environment 146, 153–163. https://doi.org/10.1016/j.atmosenv.2016.06.006

Johnson, R.L., Schmidt-Rohr, K., 2014. Quantitative solid-state13C NMR with signal enhancement by multiple cross polarization. Journal of Magnetic Resonance 239, 44–49. https://doi.org/10.1016/j.jmr.2013.11.009

Kundu, S., Kawamura, K., Andreae, T.W., Hoffer, A., Andreae, M.O., 2010. Molecular distributions of dicarboxylic acids, ketocarboxylic acids and α-dicarbonyls in biomass burning aerosols: implications for photochemical production and degradation in smoke layers. Atmospheric Chemistry and Physics 10, 2209–2225. https://doi.org/10.5194/acp-10-2209-2010

Laskin, A., Laskin, J., Nizkorodov, S.A., 2015. Chemistry of Atmospheric Brown Carbon. Chemical Reviews 115, 4335–4382. https://doi.org/10.1021/cr5006167

Lee, H.J. (Julie), Aiona, P.K., Laskin, A., Laskin, J., Nizkorodov, S.A., 2014. Effect of Solar Radiation on the Optical Properties and Molecular Composition of Laboratory Proxies of Atmospheric Brown Carbon. Environmental Science & Technology 48, 10217–10226. https://doi.org/10.1021/es502515r

Liu, S., Day, D.A., Shields, J.E., Russell, L.M., 2011. Ozone-driven daytime formation of secondary organic aerosol containing carboxylic acid groups and alkane groups. Atmospheric Chemistry

and Physics 11, 8321–8341. https://doi.org/10.5194/acp-11-8321-2011

Mao, J., Cao, X., Olk, D.C., Chu, W., Schmidt-Rohr, K., 2017. Advanced solid-state NMR spectroscopy of natural organic matter. Progress in Nuclear Magnetic Resonance Spectroscopy 100, 17–51. https://doi.org/10.1016/j.pnmrs.2016.11.003

Mao, J., Chen, N., Cao, X., 2011. Characterization of humic substances by advanced solid state NMR spectroscopy: Demonstration of a systematic approach. Organic Geochemistry 42, 891–902. https://doi.org/10.1016/j.orggeochem.2011.03.023

Mao, J., Kong, X., Schmidt-Rohr, K., Pignatello, J.J., Perdue, E.M., 2012. Advanced solid-state NMR characterization of marine dissolved organic matter isolated using the coupled reverse osmosis/electrodialysis method. Environmental Science and Technology 46, 5806–5814. https://doi.org/10.1021/es300521e

Mao, J.D., Schmidt-Rohr, K., 2004a. Accurate Quantification of Aromaticity and Nonprotonated Aromatic Carbon Fraction in Natural Organic Matter by 13C Solid-State Nuclear Magnetic Resonance. Environmental Science and Technology 38, 2680–2684. https://doi.org/10.1021/es034770x

Mao, J.D., Schmidt-Rohr, K., 2004b. Separation of aromatic-carbon13C NMR signals from di-oxygenated alkyl bands by a chemical-shift-anisotropy filter. Solid State Nuclear Magnetic Resonance 26, 36–45. https://doi.org/10.1016/j.ssnmr.2003.09.003

Mao, J.D., Xing, B., Schmidt-Rohr, K., 2001. New Structural Information on a Humic Acid from Two-Dimensional 1 H- 13 C Correlation Solid-State Nuclear Magnetic Resonance. Environmental Science & Technology 35, 1928–1934. https://doi.org/10.1021/es0014988

Martin, M., Tritscher, T., Jurányi, Z., Heringa, M.F., Sierau, B., Weingartner, E., Chirico, R., Gysel, M., Prévôt, A.S.H., Baltensperger, U., Lohmann, U., 2013. Hygroscopic properties of fresh and aged wood burning particles. Journal of Aerosol Science 56, 15–29. https://doi.org/10.1016/j.jaerosci.2012.08.006

Matos, J.T.V., Duarte, R.M.B.O., Lopes, S.P., Silva, A.M.S., Duarte, A.C., 2017. Persistence of urban organic aerosols composition: Decoding their structural complexity and seasonal variability. Environmental Pollution 231, 281–290. https://doi.org/10.1016/j.envpol.2017.08.022

McNeill, V.F., 2015. Aqueous organic chemistry in the atmosphere: Sources and chemical processing of organic aerosols. Environmental Science and Technology 49, 1237–1244.

https://doi.org/10.1021/es5043707

Minguillón, M.C., Pérez, N., Marchand, N., Bertrand, A., Temime-Roussel, B., Agrios, K., Szidat, S., van Drooge, B., Sylvestre, A., Alastuey, A., Reche, C., Ripoll, A., Marco, E., Grimalt, J.O., Querol, X., 2016. Secondary organic aerosol origin in an urban environment: influence of biogenic and fuel combustion precursors. Faraday Discuss. 189, 337–359. https://doi.org/10.1039/C5FD00182J

Mircea, M., Facchini, M.C., Decesari, S., Cavalli, F., Emblico, L., Fuzzi, S., Vestin, A., Rissler, J., Swietlicki, E., Frank, G., Andreae, M.O., Maenhaut, W., Rudich, Y., Artaxo, P., 2005. Importance of the organic aerosol fraction for modeling aerosol hygroscopic growth and activation: A case study in the Amazon Basin. Atmospheric Chemistry and Physics 5, 3111–3126. https://doi.org/10.5194/acp-5-3111-2005

Moise, T., Flores, J.M., Rudich, Y., 2015. Optical properties of secondary organic aerosols and their changes by chemical processes. Chemical Reviews 115, 4400–4439. https://doi.org/10.1021/cr5005259

Müller, A., Miyazaki, Y., Tachibana, E., Kawamura, K., Hiura, T., 2017. Evidence of a reduction in cloud condensation nuclei activity of water-soluble aerosols caused by biogenic emissions in a coolerate forest. Scientific Reports 7, 1–9. https://doi.org/10.1038/s41598-017-08112-9

Nozière, B., Kalberer, M., Claeys, M., Allan, J., D'Anna, B., Decesari, S., Finessi, E., Glasius, M., Grgić, I., Hamilton, J.F., Hoffmann, T., Iinuma, Y., Jaoui, M., Kahnt, A., Kampf, C.J., Kourtchev, I., Maenhaut, W., Marsden, N., Saarikoski, S., Schnelle-Kreis, J., Surratt, J.D., Szidat, S., Szmigielski, R., Wisthaler, A., 2015. The molecular identification of organic compounds in the atmosphere: State of the art and challenges. Chemical Reviews 115, 3919–3983. https://doi.org/10.1021/cr5003485

Padró, L.T., Tkacik, D., Lathem, T., Hennigan, C.J., Sullivan, A.P., Weber, R.J., Huey, L.G., Nenes, A., 2010. Investigation of cloud condensation nuclei properties and droplet growth kinetics of the water-soluble aerosol fraction in Mexico City. Journal of Geophysical Research 115, D09204. https://doi.org/10.1029/2009JD013195

Russell, L.M., Bahadur, R., Ziemann, P.J., 2011. Identifying organic aerosol sources by comparing functional group composition in chamber and atmospheric particles. Proceedings of the National Academy of Sciences 108, 3516–3521. https://doi.org/10.1073/pnas.1006461108

590 Sannigrahi, P., Sullivan, A.P., Weber, R.J., Ingall, E.D., 2006. Characterization of water-soluble
591 organic carbon in urban atmospheric aerosols using solid-state C-13 NMR spectroscopy.
592 Environmental Science & Technology 40, 666–672. https://doi.org/Doi 10.1021/Es051150i
593 Schmitt-Kopplin, P., Gelencsér, A., Dabek-Zlotorzynska, E., Kiss, G., Hertkorn, N., Harir, M., Hong, Y.,
594 Gebefügi, I., 2010. Analysis of the Unresolved Organic Fraction in Atmospheric Aerosols with
595 Ultrahigh-Resolution Mass Spectrometry and Nuclear Magnetic Resonance Spectroscopy:
596 Organosulfates As Photochemical Smog Constituents. Analytical Chemistry 82, 8017–8026.
597 https://doi.org/10.1021/ac101444r
598 Schmitt-Kopplin, P., Liger-Belair, G., Koch, B.P., Flerus, R., Kattner, G., Harir, M., Kanawati, B., Lucio,
599 M., Tziotis, D., Hertkorn, N., Gebefügi, I., 2012. Dissolved organic matter in sea spray: a transfer
600 study from marine surface water to aerosols. Biogeosciences 9, 1571–1582.
601 https://doi.org/10.5194/bg-9-1571-2012
602 Simoneit, B.R.T., Elias, V.O., Kobayashi, M., Kawamura, K., Rushdi, A.I., Medeiros, P.M., Rogge,
603 W.F., Didyk, B.M., 2004. Sugars - Dominant water-soluble organic compounds in soils and
604 characterization as tracers in atmospheric participate matter. Environmental Science and
605 Technology 38, 5939–5949. https://doi.org/10.1021/es0403099
606 Simpson, A.J., McNally, D.J., Simpson, M.J., 2011. NMR spectroscopy in environmental research:
607 From molecular interactions to global processes. Progress in Nuclear Magnetic Resonance
608 Spectroscopy 58, 97–175. https://doi.org/10.1016/j.pnmrs.2010.09.001
609 Suzuki, Y., Kawakami, M., Akasaka, K., 2001. 1H NMR application for characterizing water-soluble
610 organic compounds in urban atmospheric particles. Environmental Science and Technology 35,
611 2656–2664. https://doi.org/10.1021/es001861a
612 Tuet, W.Y., Fok, S., Verma, V., Tagle Rodriguez, M.S., Grosberg, A., Champion, J.A., Ng, N.L., 2016.
613 Dose-dependent intracellular reactive oxygen and nitrogen species (ROS/RNS) production from
614 particulate matter exposure: comparison to oxidative potential and chemical composition.
615 Atmospheric Environment 144, 335–344. https://doi.org/10.1016/j.atmosenv.2016.09.005
616 Verma, V., Fang, T., Guo, H., King, L., Bates, J.T., Peltier, R.E., Edgerton, E., Russell, A.G., Weber,
617 R.J., 2014. Reactive oxygen species associated with water-soluble PM2.5 in the southeastern
618 United States: spatiotemporal trends and source apportionment. Atmospheric Chemistry and
619 Physics 14, 12915–12930. https://doi.org/10.5194/acp-14-12915-2014

620 Wang, G., Kawamura, K., 2005. Molecular Characteristics of Urban Organic Aerosols from Nanjing A
621 Case Study of A Mega-City in China. Environmental Science & Technology 39, 7430–7438.
622 https://doi.org/10.1021/es051055
623 Willoughby, A.S., Wozniak, A.S., Hatcher, P.G., 2016. Detailed source-specific molecular composition
624 of ambient aerosol organic matter using ultrahigh resolution mass spectrometry and 1H NMR.
625 Atmosphere 7. https://doi.org/10.3390/atmos7060079
626 Witkowska, A., Lewandowska, A., Falkowska, L.M., 2016. Parallel measurements of organic and
627 elemental carbon dry (PM1, PM2.5) and wet (rain, snow, mixed) deposition into the Baltic Sea.
628 Marine Pollution Bulletin 104, 303–312. https://doi.org/10.1016/j.marpolbul.2016.01.003
629 Wozniak, A.S., Bauer, J.E., Dickhut, R.M., 2012. Characteristics of water-soluble organic carbon
630 associated with aerosol particles in the eastern United States. Atmospheric Environment 46,
631 181–188. https://doi.org/10.1016/j.atmosenv.2011.10.001
632 Yttri, K.E., Dye, C., Kiss, G., 2007. Ambient aerosol concentrations of sugars and sugar-alcohols at
633 four different sites in Norway. Atmospheric Chemistry and Physics 7, 4267–4279.
634 https://doi.org/10.5194/acp-7-4267-2007
635

636 **FIGURES CAPTIONS**

637

638 **Figure 1.** ^{13}C NMR with spectral editing of whole WSOM extracted from urban $PM_{2.5}$ sample S1 [(a),
639 (c), and (e)] and sample S2 [(b), (d), and (f)] collected in Aveiro. (a, b) Nearly quantitative
640 multiCP/MAS ^{13}C NMR spectra (all carbon (C)), compared to the corresponding (c, d)
641 dipolar-dephased 68-µs multiCP/MAS ^{13}C NMR spectra of nonprotonated C (C_{np}) and
642 highly mobile CH_n groups, and (e, f) selection of sp^3-hybridized C signals by a ^{13}C CSA
643 filter. The asterisk (*) in (d) denotes that the resonance at 62–94 ppm can have
644 contributions of both O-C_{np} and highly mobile O–C(H,R')–C groups.

645 **Figure 2.** 2D $^{1}H-^{13}C$ HETCOR NMR spectrum (a) and associated ^{1}H slices (b) of whole WSOM
646 extracted from $PM_{2.5}$ sample S2.

647 **Figure 3.** Structural model of aerosol WSOM in samples S1 and S2, with a ratio of aliphatic -CH_3,
648 C-CH_2-C, -COO, aromatic C-O, and anomeric O-C-O of 5:11:7:2:2 and 4:8:6:4:3,
649 respectively, as deduced from the combination of multiCP/MAS ^{13}C NMR with spectral
650 editing techniques and 2D HETCOR (R^1 to R^6 = H or alkyl group; photo: aerosol WSOM,
651 after freeze-drying).

Atmospheric Environment

Manuscript: Exploring water-soluble organic aerosols structures in urban atmosphere using advanced solid-state ^{13}C NMR spectroscopy

Authors: Regina M. B. O. Duarte*, Pu Duan, Jingdong Mao, Wenying Chu, Armando C. Duarte, Klaus Schmidt-Rohr

HIGHLIGHTS

- Advanced solid-state NMR used for the first time to decode urban aerosol WSOM
- Weekly-resolved structural data showed quantifiable changes in WSOM composition
- Accurate ambient concentrations of carbon functional groups in aerosol WSOM
- Source-specific structural characteristics for each aerosol WSOM sample
- New structural model of aerosol WSOM in contrasting atmosphere

Declaration of interests

☒ The authors declare that they have no known competing financial interests or personal relationships that could have appeared to influence the work reported in this paper.

☐The authors declare the following financial interests/personal relationships which may be considered as potential competing interests: